American Journal of Biochemistry and Biotechnology

Original Research Paper

Polymer Processing and Performance Testing Based on Kruskal Algorithm for Numerical Analysis

Yan Tang

Institute of Rail Transit, Nanjing Vocational Institute of Transport Technology, Nanjing, China

Article history
Received: 25-10-2023
Revised: 30-04-2024
Accepted: 09-05-2024

Email: amiwht2022@163.com

Abstract: Polymer processing is an injection molding product widely used in communication, medical, and other fields. The processing and forming of polymers involve complex processes, including many parameter controls to ensure the quality of finished products. This study innovatively uses the Kruskal algorithm to conduct numerical analysis on the performance of polymer processing and molding to obtain a scientifically efficient parameter setting scheme. This algorithm performs numerical analysis on polymer polymers to predict the relevant properties of finished products, thereby adjusting appropriate parameters and reducing raw material and time costs. This study conducts relevant experiments to validate it. The study considered the authenticity and reliability of the experiment and the researchers did not engage in unethical behavior during the research process, which would not affect the accuracy and credibility of the research results. Experiments showed that by introducing the Kruskal algorithm into the minimum spanning tree, the optimal selection of parameters for polymer processing and injection molding was achieved and the process could be planned. From different mold temperatures and plasticization temperatures, there was a certain variation in the tensile strength of polymer molding, but it was balanced at around 36.788MPa, with a maximum tensile degree of 37.98MPa. At this time, the mold temperature was 40°C, the plasticization temperature was 280°C and the minimum tensile strength was 35.64MPa. The mold temperature was 80°C and the plasticization temperature was 260°C. The research results show that polymer molding and parameters have high efficiency and quality. The finished product was continuously measured and the average warping variable measured was 0.5699 mm, which was very close to the predicted 0.5613 mm. The research results have developed a performance testing analysis of polymer processing and forming based on the numerical analysis of the Kruskal algorithm. This method adjusts and selects the relevant parameters and values of polymer processing and forming based on the Kruskal algorithm, quickly and effectively approaching the global optimal solution. It is suitable for products with complex geometric structures, which have high optimization efficiency. Ensuring the quality of finished products while reducing costs is of great significance for the efficient development of polymer processing and molding.

Keywords: Injection Molding, Polymer Processing, Kruskal Algorithm, Numerical Analysis

Introduction

With the rapid development of industries such as construction, automobiles, and home appliances, polymer Injection Molding (IM) plays an important role in plastic processing. IM uniformly mixes polymers and other additives, then injects them into the mold and obtains the molded product after pressure holding and cooling solidification. However, in real life, the flow properties of polymer melts and parameters such as temperature and pressure during the molding process cannot be efficiently processed using traditional formula algorithms. Traditional IM requires repeated debugging and rework, which wastes much time and raw material costs.

Therefore, algorithm optimization for IM is needed to ensure product quality and reduce time costs. To solve the cost waste and poor quality caused by improper parameters in traditional IM processes, this research adopts the Kruskal algorithm, which is an algorithm used to find the Minimum Spanning Tree (MST) of a weighted connected graph based on a greedy strategy. The basic idea of this algorithm is to perform weighted connections on connected components and then obtain the MST. This research innovatively utilizes the Kruskal algorithm's spanning tree mechanism for numerical analysis of polymer materials, predicting the related properties of finished products and adjusting appropriate parameters to reduce raw material and time costs. The parameter selection in this study aims to ensure the quality of the finished product while reducing costs, which is of great significance for the efficient development of polymer processing and forming. The research considers the authenticity and reliability of the results and the researcher does not engage in unethical behavior during the research process, which will not affect the accuracy and credibility of the research results. The structure of this study is as follows. The first elaborates on the application background of polymer and the research purpose and significance of the research algorithm. The second specifically explains the relevant performance of polymer processing and molding, as well as the process and innovation of numerical analysis on the ground of the Kruskal algorithm. The third fully elaborates on the experimental design of polymer processing and performance testing, as well as the quantitative statistics and analysis of experimental results. The fourth describes the experimental conclusions and the shortcomings of the designed method, as well as the directions for further research.

Related Works

Recently, many advanced polymer processing technologies have been developed to regulate the morphology of semi-crystalline polymers in the development of polymer processing and molding technology, such as Multi Flow Vibration IM (MFVIM). Many scholars have expressed different opinions on the development of polymer processing and molding. Gu *et al*. (2020) endowed the material with good mechanical properties, conductivity/thermal conductivity, or biomimetic structure by adjusting the processing field, namely the shear field and thermal field based on the manipulation chain orientation, crystal arrangement, or hierarchical structure distribution (Gu *et al*., 2020). This study successfully simulated the processing process of MFVIM isotactic polypropylene/high-density polyethylene parts using Moldflow by designing a special model. Alhallak *et al*. (2020) analyzed the mechanical, thermal, melt flow, and morphological behavior of Acrylonitrile Butadiene Styrene (ABS) composite materials encapsulated in bentonite. ABS/BNT composite materials were prepared using laboratory-scale micro composite materials and IM processes. The mechanical, thermomechanical, thermal, melt flow, and morphological properties of the composite were studied by tensile, hardness, and impact tests, dynamic mechanical analysis, thermogravimetric analysis, melt flow index, and scanning electron microscope (Alhallak *et al*., 2020). Lee *et al*. (2020) conducted experimental research and optimization on the Thermoplastic Resin Transfer Molding (T-RTM) process of Carbon Fiber Reinforced Thermoplastic Polymer composites (CFRTP) using a high-pressure resin transfer molding system. Then the mechanical properties, productivity, and crystal structure of the matrix and CFRTP were evaluated by differential scanning calorimetry, X-ray diffraction analysis, and tensile and inter-laminar shear strength tests. In addition, it developed a time and cost-effective flame surface treatment method. This was to remove moisture from carbon fibers and improve the interfacial bonding strength of CFRTP (Lee *et al*., 2020). Yu and his team believed that water penetration length and fiber orientation were important indicators for fiber-reinforced polymer water-assisted IM products. It was found that due to the fiber orientation and changes along the melt flow direction in water-assisted IM products, the fiber orientation in the water channel layer had the biggest and lowest changes along the melt flow direction, followed by the wall layer and finally the core layer (Yu *et al*., 2020).

Jiang *et al*. (2020) used extrusion molding technology to manufacture high-filling wood plastic composite material pallets. The effects of process parameters on mechanical properties and production stability were explored. It mixed the composite material in a twin screw extruder and then used an electronic scale for weight measurement. Before compression, this study divided it into several blocks and rearranged them in the cavity of the compression mold according to the mass distribution. The effects of compression pressure and mold temperature on bending strength, density, water absorption, and dimensional deviation were studied (Jiang *et al*., 2020). Costa *et al*. (2022) proposed a high-order accurate finite volume method to improve the numerical accuracy and computational efficiency of conjugate heat transfer simulation. Then it was applied to polymer processing. This method investigated anisotropic grids to significantly reduce the number of unknowns in convection-dominated problems. The higher temperature changes are perpendicular to curved boundaries and interfaces. The off-site data reconstruction method on the ground of polynomial reconstruction only used Polygon mesh to meet the specified boundary and interface conditions, so as to avoid the limitations of the surface mesh method (Costa *et al*., 2022). Jang combined sturdy hollow glass micro-spheres into composite materials through carefully designed screw configurations, which were suitable for processing conditions. It could be used in low-density composite materials. This study incorporated 15 parts (per 100 parts) of

sodium calcium borosilicate Hollow Glass Microspheres (HGM) into the matrix. Based on the compressive strength of HGM, the preservation rate of the microspheres and the processing conditions used for extrusion and IM were systematically checked to explore the rheological behavior of the composite material (Jang, 2020). Dekel and Kenig simulated the production of recycled polypropylene plastic particles using a 3500-ton ultra-large IM machine and Moldex3D packaging to obtain formability flow analysis. PTC Creo software was used to build plastic pallets, with a baffle cooling system filling 12 gates. In the four-stage filling process of the sequential valve gate system, the flow front diffused from the center gate to the four corners of the tray, reducing the number of welding lines and the number of gate valve openings (Dekel and Kenig, 2021).

In summary, scholars have optimized the processing of polymers or specific polymers. Different techniques are used for relevant measurement experiments. However, the research on optimizing processing performance parameters is still insufficient. Therefore, a performance testing numerical analysis method on the grounds of the Kruskal algorithm for parameter adjustment and selection is proposed, aiming to obtain more scientific and reasonable processing and forming parameters.

Materials and Methods

Polymer Processing and Forming

The performance research of polymer processing and molding needs to consider relevant basic assumptions, control equations, constitutive models, and other parameters and numerical values. This includes four stages: Injection, pressure maintaining, cooling, and mold opening processes, which are adjusted and optimized on the ground of the Kruskal algorithm for relevant parameters.

Polymer Injection Molding

The IM process is an important part of the polymer molding process. The process involves corresponding control equations, including equilibrium equations, continuity equations, and energy equations (Demay and Agassant, 2021; Galdina and Galdin, 2021). It is defined on the *xyz* coordinate axis, where *z* is the thickness direction, defined on [- *h*, *h*]. Since the melt in the pressure-maintaining stage needs to be considered as a compressible fluid to ensure the balance in the filling process, ignoring the influence of inertia force and gravity, the balance equation is a momentum equation that mainly considers the balance between pressure difference and shear force. The relevant calculations are shown in Eq. (1):

$$\begin{cases} \frac{\partial}{\partial z}\left(\eta\frac{\partial v_x}{\partial z}\right)-\frac{\partial Pr}{\partial x}=0 \\ \frac{\partial}{\partial z}\left(\eta\frac{\partial v_y}{\partial z}\right)-\frac{\partial Pr}{\partial y}=0 \\ \frac{\partial Pr}{\partial z}=0 \end{cases} \tag{1}$$

In Eq. (1), *Pr* represents the pressure. η represents the viscosity. The continuity equation is the conservation of mass equation and the relevant calculations are shown in Eq. (2):

$$\frac{\partial \rho}{\partial t}+\nabla\bullet(\rho v)=0 \tag{2}$$

In Eq. (2), *p* represents the density of the melt. *t* represents the time. $v = \{v_x, v_y, v_z\}$ represents the flow velocity of the melt in three directions. The energy equation ignores the thermal convection in the thickness direction and the thermal conduction effect in the flow direction. The relevant calculations are shown in Eq. (3):

$$\rho C_p\left(\frac{\partial T}{\partial t}+v_x\frac{\partial T}{\partial x}+v_y\frac{\partial T}{\partial y}\right)=\eta\gamma^2+k\frac{\partial^2 T}{\partial z^2} \tag{3}$$

In Eq. (3), *T* represents the temperature. *k* represents the heat conduction. γ represents the shear rate. C_p represents the heat capacity:

$$\gamma^2=\left(\frac{\partial v_x}{\partial z}\right)^2+\left(\frac{\partial v_y}{\partial z}\right)^2 \tag{4}$$

In Eq. (4), C_p and *k* are not constants, but parameters related to *T*. Due to the differences in density, heat capacity, and heat conduction between the solid and liquid phases of the melt and in the solid state, the energy equation is shown in Eq. (5):

$$\left(k_s\frac{\partial T_s}{\partial z}-k_l\frac{\partial T_l}{\partial z}\right)_{z=x}=\rho L\frac{\partial \chi}{\partial t} \tag{5}$$

In Eq. (5), *s* and *l* represent the physical properties of the polymer in both solid and liquid states. *L* represents the latent heat of material phase change. *x* represents the *z* coordinate of the solid interface. The flow velocity of the melt in the solid state is 0 and the thermal convection in the thickness direction is ignored. Therefore, the flow is symmetrical about the cavity. At the boundary of the cavity, the melt temperature is equivalent to the mold wall temperature (Du *et al*., 2021). On the ground of the above, the relevant calculations are shown in Eq. (6):

$$\begin{aligned} &v_x=v_y=0,|z|=\chi \\ &v_z=0 \\ &\frac{\partial v_x}{\partial z}=\frac{\partial v_y}{\partial z}=0,\frac{\partial T}{\partial z}=0,z=0 \\ &T=T_{mold},|z|=h \end{aligned} \tag{6}$$

During the filling and pressure-maintaining process, the melt temperature at the gate position is constant. When pressure control is used during the injection process, the

pressure at the gate is the set value. When using flow rate control, the flow rate at the gate is set. During the flow process, the pressure at the flow front is 0 and the temperature is the upstream temperature (Mohit and Selvan, 2020). Therefore, the relevant calculations are shown in Eq. (7):

$$\begin{aligned} T &= T_{gate} \\ Pr &= Pr_{gate} \\ Q &= Q_{gate} \end{aligned} \tag{7}$$

Because polymers need to construct a constitutive model during the flow process, it can be mathematically expressed as Eq. (8):

$$\tau = \eta(T, Pr, \gamma)\gamma \tag{8}$$

In addition, there are many commonly used viscosity models. This study adopts a 7 parameter cross model, which is mathematically expressed as Eq. (9):

$$\eta = \frac{\eta_0}{1+\left(\frac{\eta_0 \gamma}{\tau^*}\right)^{1-n}} \tag{9}$$

In Eq. (9), the function η_0 is shown in Eq. (10):

$$\eta_0 = D_1 \exp\left(-\frac{A_1(T-D_2-D_3Pr)}{\bar{A}_2+T-D_2}\right) \tag{10}$$

In Eq. (9), τ^* represents the material parameter. n represents the Newton's index. η_0 represents the function of T and Pr. The seven parameters are $\{\tau^*, n, D_1, D_2, D_3, A_1, \bar{A}_2\}$, which can modify the material viscosity model and describe the changes in material viscosity over a relatively large range of shear rates.

In polymer processing and molding, the state of the melt material needs to be constantly monitored. During pressure-maintaining cooling, temperature affects the density and pressure of the melt (Castillo and Barbosa, 2020; Zhang and Liu, 2021). For crystalline materials, the shrinkage of materials during the crystallization makes the state Equation suddenly change and the state Equation of amorphous materials is stable. This study uses a more reasonable dual domain Tait equation to describe the state during the crystallization process, as shown in Eq. (11):

$$\rho = V_0(T)\left(1-C\ln\left(1+\frac{Pr}{B(T)}\right)\right)+V_t(T,Pr) \tag{11}$$

There is a function calculation in Eq. (11), as shown in Eq. (12):

$$\begin{cases} V_0(T) = \begin{cases} b_{1l}+b_{2l}(T-b_5), T > T_t \\ b_{1s}+b_{2s}(T-b_5), T < T_t \end{cases} \\ B(T) = \begin{cases} b_{3l}\exp\left(-b_{4l}(T-b_5)\right), T > T_t \\ b_{3s}\exp\left(-b_{4s}(T-b_5)\right), T < T_t \end{cases} \\ V_t(T,P) = \begin{cases} 0, T > T_t \\ b_7\exp\left(-b_8(T-b_5)-b_9P\right), T < T_t \end{cases} \end{cases} \tag{12}$$

In Eq. (12), C = 1.0984. T_t represents the crystallization temperature for crystalline materials. T_t represents the glass transition temperature for amorphous materials. T_t is related to pressure P, as shown in Eq. (13):

$$T = b_5 + b_6 Pr \tag{13}$$

In Eq. (13), b_{il}, b_{is}, i = 1…4 and b_i, i = 5…9 are both material parameters. V_t (T, Pr) represents the variation term during the crystallization process. b_7 = 0 is noncrystalline materials. For crystalline and amorphous materials, specific heat is a variable parameter that cannot be ignored during IM (Hirai *et al*., 2020; Wang and Chen, 2020). It is closely related to the temperature and state of the material, as shown in Eq. (14):

$$\begin{cases} C_p(T) = C_1 + C_2(T-C_5) + C_3\tanh\left(C_4(T-C_5)\right) \\ C_p(T) = C_1 + C_2(T-C_5) + C_3\exp\left(-C_4(T-C_5)^2\right) \end{cases} \tag{14}$$

In Eq. (14), C_1, C_2, C_3, C_4, C_5 all represent material parameters. The last term represents the effect of the crystallization of latent heat on specific heat. The thermal conductivity exhibits significant performance throughout the entire IM process, with temperature having the most significant impact. If only temperature is considered, the relevant mathematical expression is shown in Eq. (15):

$$K(T) = \lambda_1 + \lambda_2(T-\lambda_5) + \lambda_3\tanh\left(\lambda_4(T-\lambda_5)\right) \tag{15}$$

In Eq. (15), λ_1, λ_2, λ_3, λ_4, λ_5 all represent material parameters.

In the IM process, the control volume method is used for simulation, which is mainly used to cut the finite element mesh of the cavity and calculate the control volume of the node according to the information of each element node (Azizi, 2021; Kamyab, 2020). IM requires the application of finite element, finite difference, control volume, and other methods to solve the pressure field, temperature field, and velocity field in the filling process. Taking the mid-plane model as an example, during the filling process, the mid-plane model undergoes 2D finite element dissection and simultaneously solves the velocity and pressure fields using finite element analysis. The element is layered on the element thickness. This study uses the finite difference method to solve the temperature field, updates the front position on the ground of the obtained

temperature field, and calculates the velocity, pressure, and temperature fields at the next moment, as shown in Fig. 1. The triangular element is defined as the flow plane in the *x* and *y* directions and the *z* direction is defined as the thickness direction. It is segmented in the thickness direction on the ground of finite element analysis.

Optimization of Polymer Forming and Numerical Analysis Method Based on Kruskal Algorithm

In the polymer processing and molding system, selecting the corresponding process parameters is extremely important, which directly affects the quality of finished product processing and molding. In this study, the MST of the Kruskal algorithm is introduced to optimally select the parameters of polymer processing and IM, plan the process, and achieve efficient and high-quality processing.

This study aims to optimize the IM process, which is a commonly used technology in polymer processing and molding. This technology can heat and melt plastic materials into an IM machine, forming a viscous polymer melt that is then sprayed into a closed mold to fill the entire cavity, maintain a certain pressure and state until cooled, and ultimately form a finished product. The IM process includes four stages: Injection, pressure maintenance, cooling, and mold opening (Zhong and Cheng, 2020; Yadav *et al*., 2020). The optimization process includes direct optimization models and indirect optimization models, mainly gate design optimization, cooling system optimization, and process parameter optimization. Gate design includes gate location, quantity, type, and shape. Increasing the number of gates appropriately can effectively reduce the flow length of the melt. The design of gate positions needs to match the number to ensure the balance of the melt in the mold cavity and the simultaneous filling of all gates.

After the filling is completed, it enters the cooling stage. To ensure the quality of the finished product, the overall temperature cooling rate needs to be consistent. Usually, the entire cooling time is over 90% of the entire production cycle. The cooling system optimization includes the design of cooling parameters and the geometric design of cooling pipes. For process parameter optimization, the main parameters include mold temperature, holding curve, injection speed, melt temperature, and cooling time (Tseng, 2023). The mold temperature is closely related to the entire processing and forming process. The injection speed and pressure are relatively balanced during the filling process, allowing the flow of the melt to overcome its resistance. If the injection speed is too low, it will lead to early condensation. If it is too high, it will cause excessive pressure in the mold cavity. However, low pressure can also lead to early cooling of the melt and the short shot. The requirements for high-pressure molding are very high. In this study, a method capable of performing IM at room temperature is designed, namely the tensile flow method (Yang and Huang, 2018), as shown in Fig. 2. This method relies on the nozzle, which changes in shape and size of the IM machine head. Before the melt enters the image, it needs to flow through a longer channel to gradually stretch the molecules inside the melt. During this process, special attention should be paid to the mold temperature to avoid the increase in melt viscosity due to hormone cooling.

The pressure-maintaining curve exhibits different changes on the ground at different pressures and times. There are mainly four types, as shown in Fig. 3. The simplest is the constant pressure maintaining curve, which is only determined by the pressure and time of pressure maintaining. If the pressure holding time is too low, the melt at the gate does not condense in time and back-flow occurs. If the time is too long, it will cause the melt at the gate to condense and have no pressure-holding effect. If the pressure maintained is too high, it will cause residual excess pressure to deform the finished product. If it is too small, it will lead to melt reflux, uneven melt shrinkage, and deformation of the finished product.

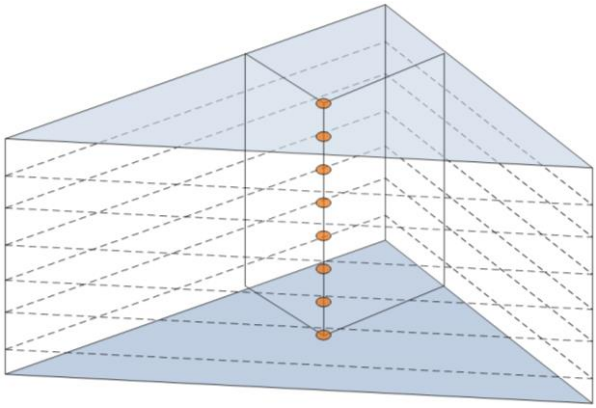

Fig. 1: Schematic diagram of finite difference grid

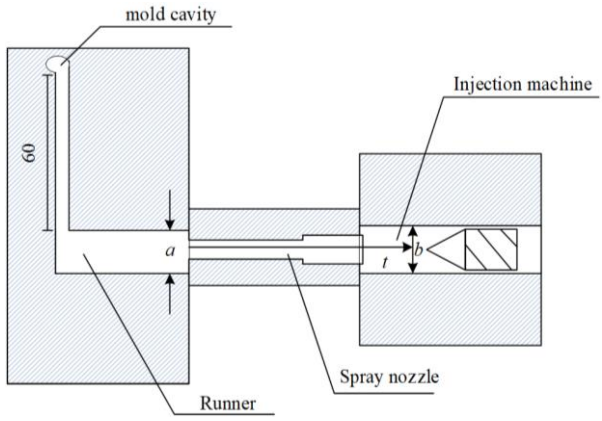

Fig. 2: Schematic diagram of the principle of obtaining self-enhancing characteristics through stretching flow

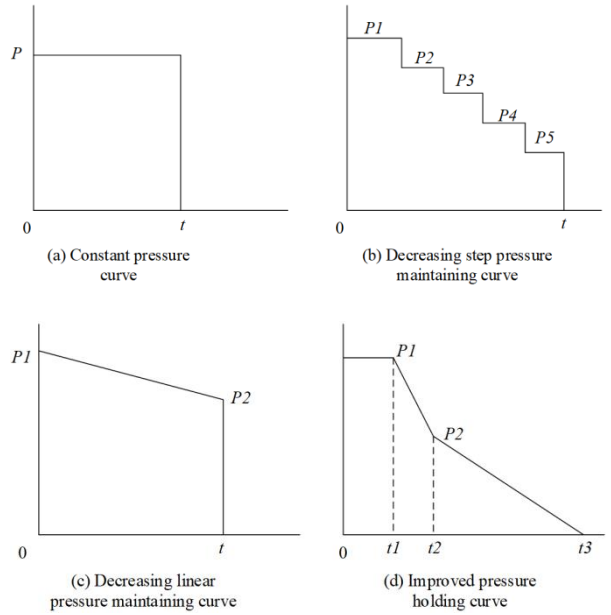

Fig. 3: Pressure holding curve

The performance numerical analysis of this study adopts the Kruskal algorithm, which is of great significance in selecting molding parameters for polymer processing. MST is a classical greedy algorithm for undirected graphs. The MST is the smallest number of the sum of the edge weights, including all the nodes of the original graph, which are connected by the smallest edge weights. The MST meets two requirements. One is that there is only one path between any fixed points and the other is that there is a connected network with n vertices. The spanning tree has only n-1 edges and n vertices (Galuppo *et al*., 2021; Bordón *et al*., 2022).

The basic idea of the Kruskal algorithm is to consider the MST from the perspective of edges. By constructing a weighted undirected graph, the fixed point is the data object in the dataset. The weighted edge is the similarity degree between data objects. Then it arranges all edges in ascending order and takes out the relevant edges in sequence. Whether the two ends of the edges can be connected in a connected component is compared. If not, it is added to the MST, and the two nodes are merged into a connected component. After repeated operations, the MST can be obtained (Song *et al*., 2018; Singh *et al*., 2019). The relevant process is shown in Fig. 4.

This research assumes that taking Fig. 5 as an example, all edges are sorted from small to large according to the weight value, such as vertex 1 and 3. They are different vertices, which can form a part of the spanning tree. It traverses all vertices and changes all colors that are the same as vertex 3 to the color of vertex 1, as shown in Fig. 5(b). Then there is the edge of vertex 4 and 6. The color marks of the vertices at both ends are different, which can become a part of the spanning tree, as shown in Fig. 5(c). The edges of the smallest vertex 3 and 6 have different color marks on both ends, which can be a part of the spanning tree. It traverses all vertices and changes the color markings of all vertices with the same color markings as vertex 6 to the color markings of vertex 1, as shown in Fig. 5(d). Similarly, it can be found that there are three edges with a weight of 5, among which vertex 1 and vertex 4 have the same color markings as vertex 3 and 4. If connected, a loop will be generated, so it is omitted. However, vertex 2 and 3 have different color markings. They can choose to change the color markings of all vertices that are the same as vertex 2 to the same color markings as vertex 3. The final result is shown in Fig. 5(f). When the number of selected edges is 1 less than the number of vertices, it is the MST.

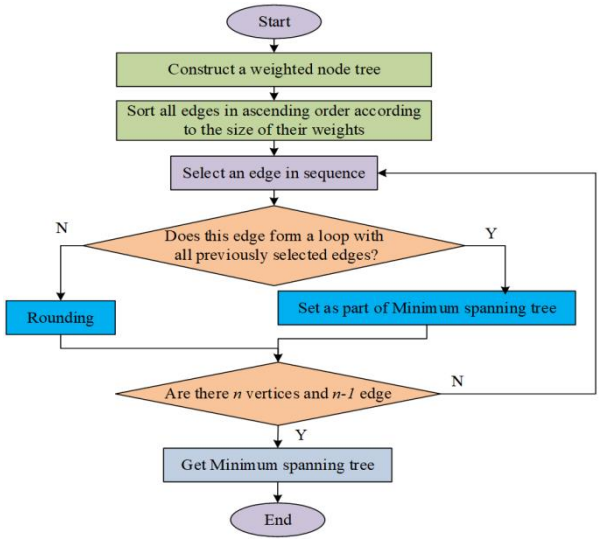

Fig. 4: Basic idea flowchart of Kruskal algorithm

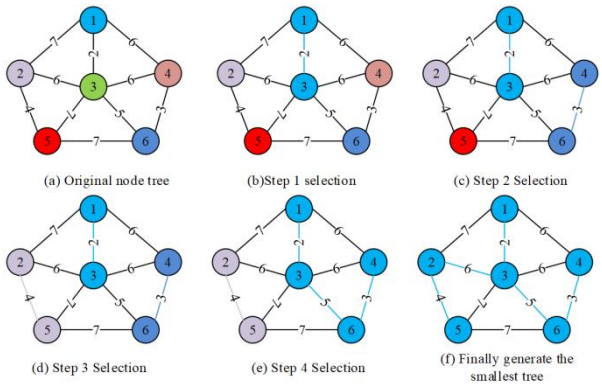

Fig. 5: The schematic diagram of the Kruskal algorithm to obtain minimum spanning tree

Results and Discussion

Experimental Study on Polymer Processing and Forming Performance Testing

Based on the processing process of polymer IM, the numerical analysis is conducted on the performance data of experimental simulation processing on the ground of the Kruskal algorithm. Then it obtains corresponding parameters to get higher-quality finished products, thereby reducing time and raw material costs.

Performance Testing Experimental Design

This experiment uses polypropylene produced by a certain brand as the experimental material, material testing, and performance parameter data (Chen *et al*., 2019; Zhao and Jiang, 2020). The relevant performance parameters include basic performance: Melt flow rate; Rheological properties: Viscosity model parameters; Physical properties: Total ash content, isotacticity, solid density, melting density, etc. Mechanical properties: Impact strength, yield strength, Rockwell hardness, etc. Thermal performance: Thermal deformation temperature, thermal conductivity, specific heat, etc., as shown in Table 1.

To visually demonstrate the experimental process, the basic route is shown in Fig. 6. It uses Mold flow to simulate the sample formation, ensuring smooth processing in the experiment. The simulation results depend on the calculation model and the setting of various parameters. It is necessary to use visualization equipment to observe the flow state of the melt injection process in the mold cavity and obtain the flow velocity of the melt front through a high-speed camera. It obtains different simulation results on the ground of parameter adjustments.

Experimental Result Data Statistics and Quantitative Analysis

The temperature data for this study is shown in Table 2, which records and calculates different mold temperatures, plasticizing temperatures, injection speeds, and tensile strength of the finished product. This indicates that when the mold temperature was 40°C, the injection speed was 20 cm^3/s and the plasticization temperature was 280°C. The tensile strength of the polymer after molding was the highest, at 37.98MPa. When the mold temperature was 40°C, the injection speed was 15 cm^3/s and the plasticization temperature was 240°C. The tensile strength of the polymer after molding was the smallest, which was 35.64MPa.

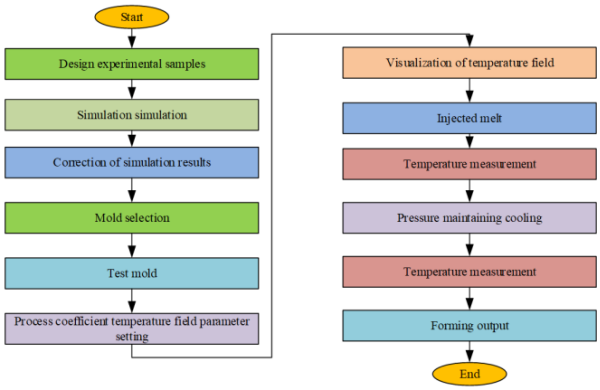

Fig. 6: Basic route and process of research

Table 1: Polypropylene material testing data and performance parameters

Performance items		Test data	Unit	Performance parameter	Indicator items	Parameter value
Basic performance	Melt flow rate	2.95-3.61	g/10 min	Rheological properties	Viscosity model parameters	n = 0.23565; τ^* = 34934.5 *Pa;* $D_1 = 4.64 \times 10^{20} Pa.s$ D_2 = 263.25 *K,* D_3 = 0*K/ Pa*; A_1 = 44.41, A_2 = 28.40 *K*
Physical property	Isotacticity	95.5-97.0	%	Physical property	Solid density	0.7751g/cm^3
	Total ash content	132			Melt Density	0.92889g/cm^3
Mechanical properties	Impact strength	5	kg•cm/cm		Transition temperature	135°C
	Flexural modulus	15100	kg/cm^2		Degradation temperature	330°C
	Tensile yield strength	360	kg/cm^2	Mechanical property	Elastic modulus	2340 MPa
	Rockwell hardness	88	R		Shear modulus	482.29 MPa
Thermal performance	Heat distortion temperature	94	°C	Thermal performance	Thermal conductivity coefficient	0.229W/°C (215.44°C)
	Vicat softening point	151	°C		Specific heat	3200J/kg°C (254.5°C)

DOI: 10.3844/ajbbsp.2024.197.207

Table 2: Tensile strength data under different mold temperatures, plasticizing temperatures, and injection speeds

Group number	Mold temperature/°C	Plasticization temperature/°C	Injection speed/cm³/s	Polymer forming tensile strength/MPa
1	40	240	15	35.64
2	40	240	20	36.71
3	40	260	15	36.67
4	40	260	20	37.54
5	40	280	15	37.86
6	40	280	20	37.98
7	80	240	15	36.34
8	80	240	20	35.76
9	80	260	15	36.15
10	80	260	20	35.68
11	80	280	15	37.61
12	80	280	20	37.52
13	60	240	15	34.65
14	70	240	15	35.29
15	80	240	15	35.92
16	90	240	15	36.12
17	100	240	15	36.59
18	115	240	15	36.88

To more intuitively display the tensile strength of polymer molding, the above data is converted using a bar statistical chart, as shown in Fig. 7. This indicated that with the increase of mold temperature, plasticization temperature, and injection speed, the tensile strength of polymer molding varied to a certain extent, but it was balanced at around 36.788 MPa, with the maximum tensile strength of 37.98 MPa and the minimum tensile strength of 35.64 MPa. The group with a mold temperature of 40°C and a mold temperature of 80°C showed a certain upward and downward trend with temperature and elongation, respectively. The average tensile strength of the 40°C mold temperature experimental group increased from 36.72-37.41 MPa with the increase in plasticization temperature. The average tensile strength of the 80°C mold temperature experimental group decreased from 36.7-36.32 MPa as the plasticizing temperature increased. However, in the group with a mold temperature of 80°C, the plasticization temperature increased from 240-260°C, resulting in a relatively significant decrease in tensile strength. On the other hand, in the group with a mold temperature of 40°C, there was a significant improvement in tensile strength.

In Fig. 8, the mold flow is used to predict the temperature field of melt flow. Fig. 8(a) shows the line chart diagram of temperature field prediction with the plasticizing temperature of 240°C, mold temperature of 40, and 80 °C, and injection speed of 15 and 20 cm³/s. Fig. 8(b) shows the line chart diagram of temperature field prediction with the plasticizing temperature of 260°C, mold temperature of 40 and 80°C, and injection speed of 15 and 20 cm³/s. This indicates that the plasticization temperature increases as the distance from the midpoint increases after the melt enters the mold cavity. A high injection speed indicates a higher temperature in the mold cavity. When the injection speed was relatively low, the temperature increased by 2°C. When the injection speed was high, the temperature increased by about 3°C.

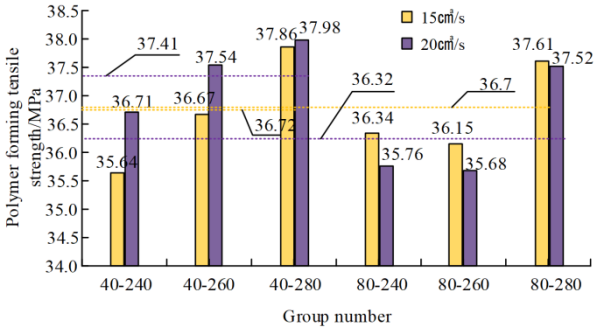

Fig. 7: The tensile strength of the finished product under different mold temperatures, plasticizing temperatures, and injection speeds

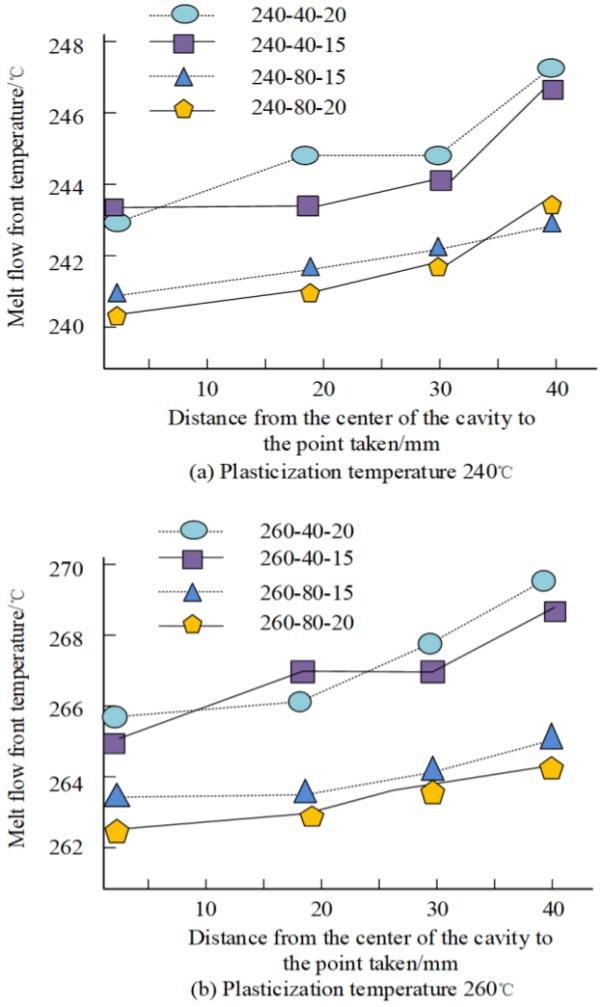

Fig. 8: Predicting data on the temperature field of melt flow

To clarify the temperature of various parts of the mold more clearly, sensors are installed at three positions on the gate. Figure 9(a) shows the relevant temperature test results of the sensor. Figure 9(b) shows the measurement results of the inlet gate, the far gate, and the center of the

gate after several experiments. After conducting six experiments, the cooling trend at the gate during cooling is mostly normal and uniform, ranging from a maximum of 171°C to a minimum of 147°C. The temperature increased as the distance from the gate decreased.

In the experiment, the injection molded samples are measured. The average analysis of the experimental factor levels, namely the holding time and cooling time, is refined to obtain the relevant degree of warping deformation, which is convenient for analyzing the molding process performance. The specific experimental statistical process is shown in Table 3.

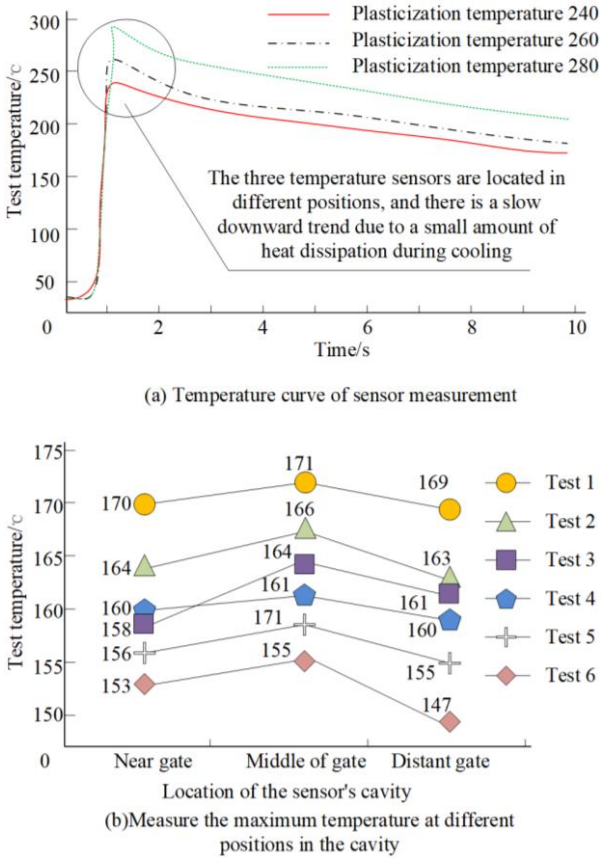

Fig. 9: Temperature testing of sensors at different gate locations

Table 3: The specific experimental statistical process of the degree of warping deformation

Holding temperature	Cooling time	Curling degree
4.152	4.301	0.5701
4.226	4.329	0.5703
4.325	4.361	0.5732
4.451	4.399	0.5729
4.522	4.514	0.5722
4.611	4.496	0.5714
4.632	4.625	0.5712
4.696	4.799	0.5711
4.756	4.654	0.5874
4.816	4.686	0.5705

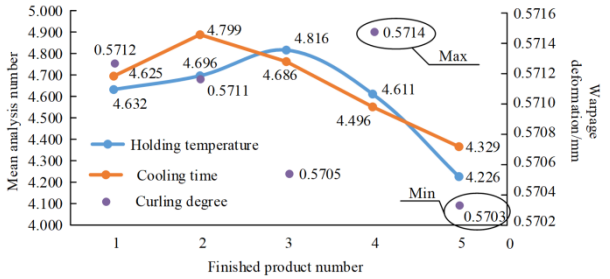

Fig. 10: Mean analysis data of holding time and cooling time, as well as curling deformation data

Figure 10 shows the curl deformation data and mean analysis data of 5 finished products. From the mean analysis, when the experimental factor level holding time was 4.611 sec and the cooling time was 4.496 sec, the maximum warping deformation reached 0.5714 mm. When the holding time at the experimental factor level was 4.226 sec and the cooling time was 4.329 sec, the minimum warping deformation was 5703 mm. During the experimental process, the finished product was continuously measured and the average measured warping variable was 0.5699 mm, which was very close to the predicted 0.5613 mm. This indicated the practicality and feasibility of the algorithm in this study.

Conclusion

The processing and molding of polymer is an inevitable result of the rapid development of various industries today. To improve the efficiency of polymer processing and molding, ensure the quality of finished products, and reduce raw material and time costs, this study proposed the optimal selection of process performance parameters on the ground of the Kruskal algorithm. Relevant experiments were conducted to test the relevant performance. The experiment showed that at the average analysis level and experimental factor level, the maximum warping deformation reached 0.5714 mm, the insulation time was 4.611 and the cooling time was 4.496. When the experimental factor level holding time was 4.226 and the cooling time was 4.329, the minimum warping deformation was 5703 mm. Therefore, the polymer processing on the ground of the above plan was selected and the finished product was continuously measured. The average measured warping deformation was 0.5699 mm, which is very close to the predicted 0.5613 mm. This indicates that the parameter selection of the algorithm in this study is of great significance for the efficient development of polymer processing and molding while ensuring the quality of the finished product. However, the impact parameters of this study are relatively small. A system optimization model considering gate position, cooling system, and process parameters is

proposed for the optimization design of the polymer forming process. In practical problems, other design indicators often need to be considered, such as gate quantity, type and shape, hot runner design, product thickness, and material parameters. Therefore, the performance test results have certain limitations, which require parameter expansion in subsequent research to obtain more accurate and scientific processing parameter schemes. This study received funding from the 2022 Jiangsu Province "Qinglan Project". Thanks for the strong support provided by the "Qinglan Project" in 2022, which has helped researchers make significant progress in experimental materials, equipment procurement, and data analysis.

Acknowledgment

This study was funded by the "Qinglan Project" in Jiangsu Province in 2022. Thank you for the strong support provided by the 2022 Qinglan Project, which has helped researchers make significant progress in experimental materials, equipment procurement, and data analysis.

Funding Information

The research is supported by Jiangsu province's "Qinglan project" in 2022.

Ethics

This article does not contain any studies with human participants performed by any of the authors.

Reference

Alhallak, L. M., Tirkes, S., & Tayfun, U. (2020). Mechanical, thermal, melt-flow, and morphological characterizations of bentonite-filled ABS copolymer. *Rapid Prototyping Journal*, *26*(7), 1305–1312. https://doi.org/10.1108/rpj-12-2019-0321

Azizi, M. (2021). Atomic orbital search: A novel metaheuristic algorithm. *Applied Mathematical Modelling*, *93*, 657–683. https://doi.org/10.1016/j.apm.2020.12.021

Bordón, P., Elduque, D., Paz, R., Javierre, C., Kusić, D., & Monzón, M. (2022). Analysis of processing and environmental impact of polymer compounds reinforced with banana fiber in an injection molding process. *Journal of Cleaner Production*, *379*, 134476. https://doi.org/10.1016/j.jclepro.2022.134476

Castillo, L. A., & Barbosa, S. E. (2020). Influence of processing and particle morphology on final properties of polypropylene/talc nanocomposites. *Polymer Composites*, *41*(8), 3170–3183. https://doi.org/10.1002/pc.25608

Chen, J.-Y., Liu, C.-Y., & Huang, M.-S. (2019). Enhancement of Injection Molding Consistency by Adjusting Velocity/Pressure Switching Time-Based on Clamping Force. *International Polymer Processing*, *34*(5), 564–572. https://doi.org/10.3139/217.3867

Costa, R., Nóbrega, J. M., Clain, S., & Machado, G. J. (2022). High-order accurate conjugate heat transfer solutions with a finite volume method in anisotropic meshes with application in polymer processing. *International Journal for Numerical Methods in Engineering*, *123*(4), 1146–1185. https://doi.org/10.1002/nme.6892

Dekel, Z., & Kenig, S. (2021). Micro-Injection Molding of Polymer Nanocomposites Composition-Process-Properties Relationship. *International Polymer Processing*, *36*(3), 276–286. https://doi.org/10.1515/ipp-2020-4065

Demay, Y., & Agassant, J. F. (2021). The Polymer Film Casting Process – An Overview. *International Polymer Processing*, *36*(3), 264–275. https://doi.org/10.1515/ipp-2020-4061

Du, X.-L., Jin, J.-B., Long, X.-B., Xiong, Y.-M., & Song, J.-L. (2021). Effect of Graphene, SiO_2 and Zeolite Powder on the Mechanical and Scratch Properties of PP. *International Polymer Processing*, *36*(1), 44–52. https://doi.org/10.1515/ipp-2020-3965

Galdina, V. D., & Galdin, N. S. (2021). Polymer-Bitumen Binders Compositions Selection by Using the Experimental Planning Method. *Key Engineering Materials*, *887*, 504–510. https://doi.org/10.4028/www.scientific.net/kem.887.504

Galuppo, W. de C., Magalhães, A., Ferrás, L. L., Nóbrega, J. M., & Fernandes, C. (2021). New boundary conditions for simulating the filling stage of the injection molding process. *Engineering Computations*, *38*(2), 762–778. https://doi.org/10.1108/ec-04-2020-0190

Gu, X., Hong, R., Leng, J., Hu, M., Fu, Q., & Zhang, J. (2020). Evolution of iPP/HDPE Morphology under Different Mold Temperatures via Multiflow Vibration Injection Molding: Thermal Field Simulation and Oriented Structures. *Industrial and Engineering Chemistry Research*, *59*(14), 6741–6750. https://doi.org/10.1021/acs.iecr.0c00097

Hirai, H., Oshiro, R., & Tanaka, K. (2020). Counting Integral Points in Polytopes via Numerical Analysis of Contour Integration. *Mathematics of Operations Research*, *45*(2), 455–464. https://doi.org/10.1287/moor.2019.0997

Jang, K.-S. (2020). Low-density polycarbonate composites with robust hollow glass microspheres by tailorable processing variables. *Polymer Testing*, *84*, 106408. https://doi.org/10.1016/j.polymertesting.2020.106408

Jiang, T., Zeng, G., & Hu, C. (2020). Fabrication of highly filled wood plastic composite pallets with extrusion-compression molding technique. *Polymer Composites*, *41*(7), 2724–2731. https://doi.org/10.1002/pc.25570

Kamyab, G.-R. (2020). Optimal Feeder Routing and DG Placement Using Kruskal's Algorithm. *European Journal of Electrical Engineering*, *22*(1), 71–78. https://doi.org/10.18280/ejee.220109

Lee, J., Lim, J. W., & Kim, M. (2020). Effect of thermoplastic resin transfer molding process and flame surface treatment on mechanical properties of carbon fiber reinforced polyamide 6 composite. *Polymer Composites*, *41*(4), 1190–1202. https://doi.org/10.1002/pc.25445

Mohit, H., & Selvan, V. A. M. (2020). Effect of a Novel Chemical Treatment on the Physico-Thermal Properties of Sugarcane Nanocellulose Fiber Reinforced Epoxy Nanocomposites. *International Polymer Processing*, *35*(2), 211–220. https://doi.org/10.3139/217.3855

Singh, A. K., Siddhartha, & Yadav, S. (2019). Mechanical and Fracture Peculiarities of Polypropylene-Based Functionally Graded Materials Manufactured via Injection Molding. *International Polymer Processing*, *34*(5), 573–585. https://doi.org/10.3139/217.3784

Song, M. C., Liu, Y., & Chang, H. (2018). Development of High Pressure Injection Technology for Normal Hydraulic Injection Molding Machines. *International Polymer Processing*, *33*(1), 52–59. https://doi.org/10.3139/217.3364

Tseng, H.-C. (2023). Numerical visualization of extensional flows in injection molding of polymer melts. *International Polymer Processing*, *38*(2), 175–182. https://doi.org/10.1515/ipp-2022-4316

Wang, Y., & Chen, Y. (2020). Shifted Legendre Polynomials algorithm used for the dynamic analysis of viscoelastic pipes conveying fluid with variable fractional order model. *Applied Mathematical Modelling*, *81*, 159–176. https://doi.org/10.1016/j.apm.2019.12.011

Yadav, H., Kumari, A. C., & Chhikara, R. (2020). Feature selection optimisation of software product line using metaheuristic techniques. *International Journal of Embedded Systems*, *13*(1), 50–64. https://doi.org/10.1504/ijes.2020.108284

Yang, Y.-J., & Huang, C.-C. (2018). Effects of ultrasonic injection molding conditions on the plate processing characteristics of PMMA. *Journal of Polymer Engineering*, *38*(9), 905–914. https://doi.org/10.1515/polyeng-2018-0004

Yu, Z., Liu, H., Kuang, T., Huang, X., Chen, Z., Zhang, W., & Zhang, K. (2020). The study of short-shot water-assisted injection molding of short glass fiber reinforced polypropylene. *Journal of Applied Polymer Science*, *137*(47), 49555. https://doi.org/10.1002/app.49555

Zhang, H., & Liu, X. (2021). Numerical analysis of the flow and heat transfer characteristics in serpentine microchannel with variable bend amplitude. *International Journal of Numerical Methods for Heat & Fluid Flow*, *31*(6), 2022–2041. https://doi.org/10.1108/hff-06-2020-0334

Zhao, W., & Jiang, Z. (2020). Research on Occupational Health and Safety of Medical Staff Based on ISO 45001. *American Journal of Biochemistry and Biotechnology*, *16*(3), 288–298. https://doi.org/10.3844/ajbbsp.2020.288.298

Zhong, X., & Cheng, P. (2020). An Improved Differential Evolution Algorithm Based on Dual-Strategy. *Mathematical Problems in Engineering*, *2020*, 1–14. https://doi.org/10.1155/2020/9767282